

Table 4 Second-stage empty weight trades; first-stage depletion cutoff

| For $G =$ | $\partial W_{E2}/\partial G_1 =$ | $\partial W_{E2}/\partial G_2 =$ |
|-----------|-----------------------------------|----------------------------------|
| W_{LP} | $\xi\beta_1(1 + \xi)^{-1}$ | $(\beta_2 - \xi)(1 + \xi)^{-1}$ |
| I_{sp} | $m_2(1 + \xi)^{-1} \ln \mu_1$ | $m_2(1 + \xi)^{-1} \ln \mu_2$ |
| W_R | $-\xi u_1 \beta_1 (1 + \xi)^{-1}$ | $-u_2 \beta_2 (1 + \xi)^{-1}$ |
| W_I | $-\xi(1 + \xi)^{-1}$ | 0 |

margin. The method used to derive the tradeoffs is similar to that of Ref. 1; the results are basically an extension of that work. The expressions are approximate in that gravity and drag losses are neglected in the derivation, but the accuracy is sufficient for many purposes (see Table 1).

The expressions for the approximate tradeoffs are found from the differentials of the defining equations (1-5) and from the statement that the total characteristic velocity is held fixed:

$$dV_{total} = d(V_1 + V_2) \equiv 0 \quad (9)$$

or

$$0 = d(gI_{sp1} \ln \mu_1 + gI_{sp2} \ln \mu_2) \quad (10)$$

Equation (10) becomes:

$$I_{sp1} \left[\frac{dW_{01}}{W_{01}} - \frac{dW_{BO1}}{W_{BO1}} + \frac{dI_{sp1}}{I_{sp1}} \ln \mu_1 \right] + I_{sp2} \left[\frac{dW_{02}}{W_{02}} - \frac{dW_{BO2}}{W_{BO2}} + \frac{dI_{sp2}}{I_{sp2}} \ln \mu_2 \right] = 0 \quad (11)$$

Let

$$\beta \equiv (\mu - 1)^{-1} \quad (12)$$

Then

$$(\mu\beta)^{-1} = W_P/W_0 = \text{propellant fraction} \quad (13)$$

Finally, let

$$m \equiv W_0\beta/I_{sp} \quad (14)$$

The resulting tradeoffs (or influence coefficients, which are partials with respect to G , where $G = W_{LP}$, I_{sp} , etc.) for single-stage vehicles are shown in Tables 2 and 3. The existence of two sets of burnout weight trades shows the need to specify either constant margin or empty weight.

Two-stage trades fall into two categories:

1) The first stage is programed for a "depletion cutoff," and it can be low in cutoff velocity; the deficiency is made up by the second stage. Second-stage empty weight and margin tradeoffs on this basis are shown in Tables 4 and 5, respectively.

To shorten the expressions, the parameter ξ is defined:

$$m_2/m_1 \equiv \xi = W_{02}\beta_2 I_{sp1}/W_{01}\beta_1 I_{sp2} \quad (15)$$

2) The first stage is programed for a "guidance cutoff"; it has a propellant margin and a constant cutoff velocity. Then the one-stage trades in Tables 2 and 3 are applicable to the second stage. In addition:

$$\partial W_{E2}/\partial W_{D1} = -\mu_2^{-1} \quad \partial W_{M2}/\partial W_{D1} = -(\mu_2\beta_2)^{-1}$$

More accurate trades for the booster phase may be found by the methods of Ref. 2.

Table 5 Second-stage margin trades; first-stage depletion cutoff

| For $G =$ | $\partial W_{M2}/\partial G_1 =$ | $\partial W_{M2}/\partial G_2 =$ |
|-----------|---------------------------------------|-------------------------------------|
| W_{LP} | $\xi\beta_1(\mu_2\beta_2)^{-1}$ | $u_2^{-1} - \xi(\mu_2\beta_2)^{-1}$ |
| I_{sp} | $m_2(\mu_2\beta_2)^{-1} \ln \mu_1$ | $m_2(\mu_2\beta_2)^{-1} \ln \mu_2$ |
| W_R | $-\xi(u_1\beta_1)(\mu_2\beta_2)^{-1}$ | -1 |
| W_I | $-\xi(\mu_2\beta_2)^{-1}$ | |
| W_E | ... | $-(1 + \xi)(\mu_2\beta_2)^{-1}$ |

References

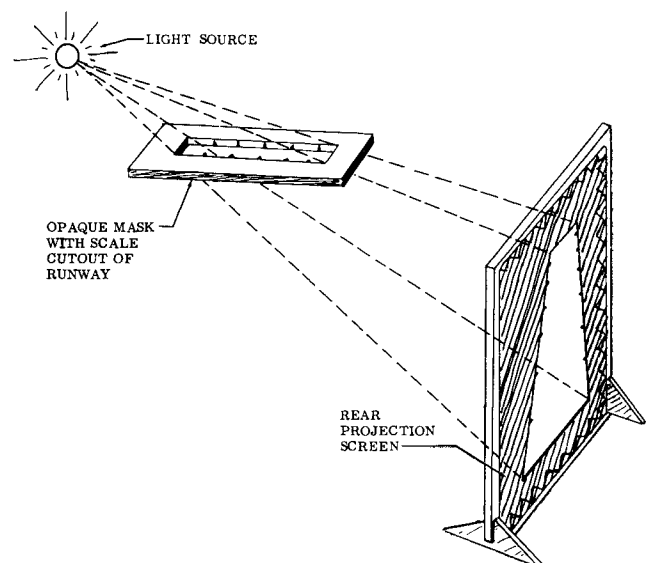
- Geckler, R. D., "Ideal performance of multi-stage rockets," ARS J. **30**, 531-535 (1960).
- Pollak, R. J., "Rapid determination of the interactions between a ballistic rocket and its trajectory," ARS J. **32**, 42-51 (1962).

TV Missile Terminal-Flight Simulator

LEROY P. LOPRESTI* AND G. FRED DUNMIRE†
Grumman Aircraft Engineering Corporation,
Bethpage, N. Y.

A SIMULATOR display designed and built by Grumman specifically for the evaluation of missile control systems in which an operator "flies" the missile by a control stick while watching the target area on television is described. A mechanical/optical device, driven by an analog computer, projects the target area on a screen, which is viewed by closed-circuit TV. The terrain in the target area is realistically displayed, in correct perspective for the missile's instantaneous position and altitude. Each flight terminates when the missile impacts the ground. This synthetic display can be used to determine miss-distance sensitivity to gusts, winds, missile speed, optical axis orientation and field of view, aerodynamic and dynamic factors, and control-system mechanization (e.g., strapped-down or gimbaled camera, rate, or position autopilot).

The terminal-flight simulator was designed to meet the following requirements: 1) TV presentation of the terrain seen during the terminal phase, viewed in correct perspective for the missile's instantaneous location and attitude; 2) six degrees of freedom at response levels well above those expected of an actual missile; 3) flight-path versatility enabling the operator to fly various trajectories; and 4) an inexpensive, easily changed, realistic terrain model.

**Fig. 1 Runway projection.**

Presented at the AIAA Simulation for Aerospace Flight Conference, Columbus, Ohio, August 26-28, 1963 (no preprint number; published in bound volume of preprints of the meeting); revision received March 9, 1964.

* Missile Project Engineer; now G.S.E. Resident Representative at the Atlantic Missile Range. Member AIAA.

† Assistant manager, Advanced Systems. Member AIAA.

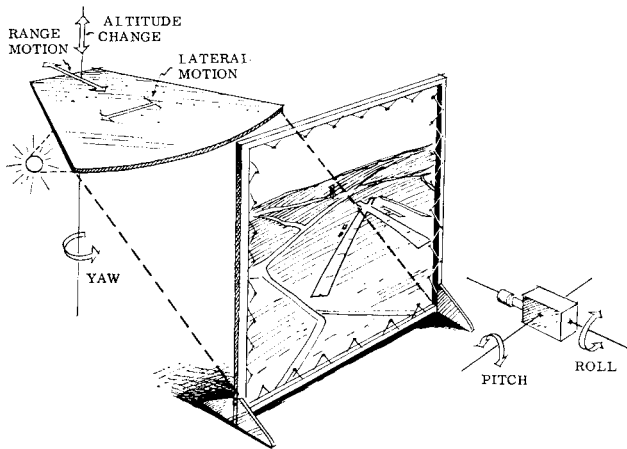


Fig. 2 Schematic illustrating projection geometry with reflector and six degrees of freedom.

The manner in which perspective and "flight" to impact are obtained, without a focus problem at short range, can be described as follows. If a scale model of an airport runway is viewed from a scale altitude and range, the perspective obtained by the viewer is the same as that which he would see were he actually aboard a missile in flight toward the runway. If the viewer's eye is replaced by a light source, and the scale model is replaced by a mask cut from opaque material, an image of the runway can be projected on a vertical screen, as shown in Fig. 1. If this projected image is now viewed from the opposite side of the screen, at a distance equal to the light-to-screen distance, and on the line which passes through the light source and is perpendicular to the screen, a one-to-one geometry analog will exist—an eye at the new viewing point will see the runway on the screen exactly as it would see the runway mask from the light-source point. Furthermore, if the runway mask is moved (relative to the fixed light source) by an analog computer at linear and angular rates that correspond to the scale of the runway model and the particular missile being simulated, the viewer will see the projected runway moving exactly as it would for the missile in flight. If the missile is "flown" toward a target symbol on the runway, the computer will drive the mask toward the light source, and the physical distance between the light source and the target symbol will decrease continuously to zero. However, the viewer (a TV camera) sees the projected image on the screen, and, since the distance to the screen remains constant, large range changes are provided without a focusing problem.

A runway mask has been used to describe the projection technique only because this simple shape lends itself to per-

spective illustration. The system just described could be provided with a vertical-view transparency of any random-textured target area; however, use of a transparency can cause a serious limitation due to partial reflections at shallow illumination angles. A better technique is to use a large opaque reflector surface with the light source on the other side (Fig. 2).

The viewing geometry in Fig. 2 is the same as that for the runway mask, except that the TV camera must now be placed on a line which passes through the virtual light point, i.e., the point at which the light source would have been placed for a mask, as in Fig. 1, and is perpendicular to the screen. The reflector is provided with vertical, longitudinal, lateral, and yawing motions, and the TV camera is provided with pitch and roll motions, giving a total of six degrees of freedom. For an altitude change, the reflector and the light source are moved simultaneously, with the bulb moving at twice the reflector's rate, so that the *virtual light source is kept at a fixed position*. The nodal point of the lens system of the TV camera is the view point; rotating the camera around the nodal point produces no change in perspective of the target area as seen on the TV monitor.

In practice, it is mechanically advantageous to invert the terrain drive mechanism (and the image on the screen), as in Fig. 3. The terrain image is then re-inverted in the closed-circuit TV system, so that the operator sees the erect image (as illustrated by the photograph of Fig. 4). He commands the missile with a fingertip controller. A separate light provides a horizon and sky.

Since the light source is the analog of the TV camera's location relative to the terrain reflector, it must actually contact the reflector surface to simulate flight to impact. The light source is an arc within a glass bulb that prevents the arc from touching the reflector. To eliminate this restriction, a lens system focuses the light to a small spot outside the bulb. Flight to impact is provided by driving this apparent point light-source toward the reflector until it actually impinges upon the surface.

The terrain reflector is Alzac, a highly reflective sheet of aluminum, on which terrain features such as coastline, roads, and random-textured fields are painted. Those areas that are to appear light (such as concrete roads and water) are left unpainted. Shades of gray are obtained by spraying non-reflective black paint in different densities. Areas to appear dark are painted black. The realism obtained with this reflector is illustrated by the photograph in Fig. 4. Some three dimensionality can be provided. Objects such as water towers and radar antennas are legitimately displayed.

The miss distance is the minimum separation that occurs between the light and the target during the terminal phase of flight. This distance is measured by three potentiometers mechanically attached to the reflector and driven by reflector motion. Their outputs feed two $x-y$ recorders that

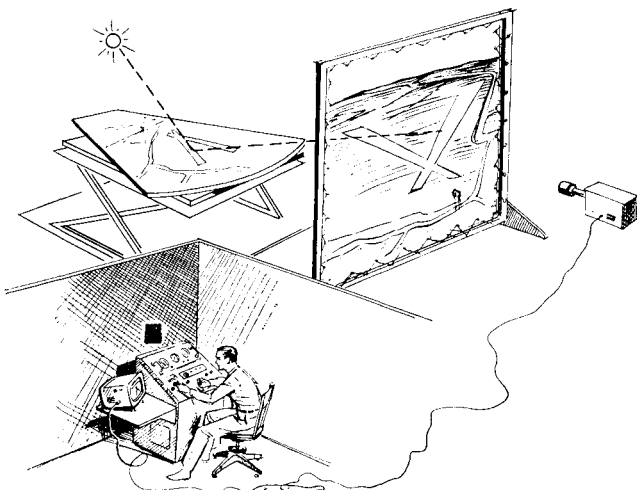


Fig. 3 Simulator general arrangement.

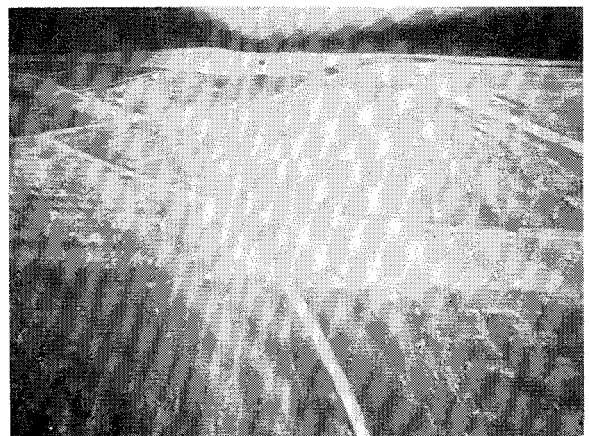


Fig. 4 Terrain display.

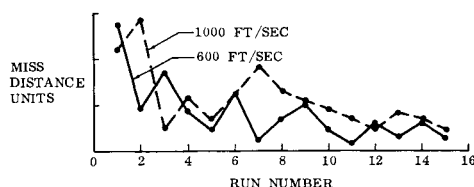


Fig. 5 Learning curves for operators flying missiles at fixed velocities indicated; modified four-degree-of-freedom program.

plot the missile's path projected in horizontal and vertical planes passing through the center of the target. The recorders are optically indexed (zero miss distance) to the target on the scale terrain by driving the reflector to the point at which light source and the center of the target are coincident and by zeroing the recorder pens. A scale of 1 in. of pen movement per 50 ft of missile travel provides very accurate miss-distance measurements but limits the recording to the final 500 ft of the trajectory. However, a continuous strip recorder documents the entire flight-path geometry, body attitude and rates, gusts, and load factors.

Initial flight-control experiments employed a modified four-degree-of-freedom program with simple manual-control systems. Missiles were flown at constant speed and zero roll angle in a wings-level, yaw-to-turn mode. Typical learning curves for two missile speeds are shown in Fig. 5. The miss distances shown are due primarily to error in vertical path, which was more difficult for the operators to control than lateral path; after 15 runs the operators were able to fly the missile with consistent accuracy. This program is continuing with more difficult tests, including effects of cross winds and random gusts.

Space Propulsion by Magnetic-Field Interaction

J. F. ENGELBERGER*

Consolidated Controls Corporation, Bethel, Conn.

Introduction

A MAGNETIC dipole experiences no net translational force in a uniform magnetic field. Instead, the dipole senses a couple until its axis is parallel to the lines of force of the field. On the other hand, in a nonuniform field, the translational force on a dipole in cartesian coordinates can be expressed as follows:

$$F_x = M_x \frac{\partial H_x}{\partial x} + M_y \frac{\partial H_y}{\partial x} + M_z \frac{\partial H_z}{\partial x}$$

$$F_y = M_x \frac{\partial H_x}{\partial y} + M_y \frac{\partial H_y}{\partial y} + M_z \frac{\partial H_z}{\partial y}$$

$$F_z = M_x \frac{\partial H_x}{\partial z} + M_y \frac{\partial H_y}{\partial z} + M_z \frac{\partial H_z}{\partial z}$$

where F is the force, M the dipole movement, and H the magnetic field.

The contention will be made herein that space is permeated with nonuniform magnetic fields and that a dipole of signifi-

cant magnetic strength will experience accelerating forces of practical magnitude. In a space propulsion system, the dipole is created by means of a current-carrying loop of wire. If this loop is operated as a superconductor, it offers interesting possibilities in efficient space propulsion. The key consideration, whether or not a superconductor is used, is to develop propulsive thrust without dissipating the mass of the space vehicle.

Magnetic-field interaction space propulsion can be likened to sailing uncharted seas while being steered by the winds. The space-sailor captain will have to learn the changing pattern of magnetic fields and to find the maximum gradients, so that he can make use of these forces to propel him on his way. He will enjoy one ancillary advantage from dipole propulsion. Charged particles will be deflected from their normal deadly path when entering the domain of the dipole. Not very much information is available on magnetic fields in space beyond a few geocentric radii of the earth. We know of bands of charged particles around the earth, and we have measured anomalies resulting from particles arriving from the sun. Generally, these factors tell of sharp gradients in the earth's magnetic field. The shrewd space mariner will seek out such gradients for that extra kick.

The earthbound speculator can, however, ignore the anomalies and concentrate on the earth as a giant magnetic dipole. This dipole creates a nonuniform magnetic field. It will be shown that the gradient of this field is sufficient to justify consideration of dipole magnetic-field interaction as a means of propulsion for accelerating the already orbiting vehicle up to escape velocity. That much is claimed for the ion propulsion system, and that system must dissipate its substance in developing acceleration.

Dipole Propulsive Force in Earth's Magnetic Field

In Fig. 1 is shown a dipole, represented by a single loop, which is located at some distance from the earth's surface commensurate with its being in a stable orbit. The net translational force can be expressed as follows:

$$\vec{F} = \frac{5 \times 10^{-11} N I A}{\xi^4} \left[-\hat{r} - (\cos \beta \cos \theta + \frac{1}{2} \sin \beta \sin \theta) + \theta \left(-\frac{1}{3} \cos \beta \sin \theta + \frac{1}{6} \sin \beta \sin \theta \right) \right] \quad (1)$$

where N is the number of turns in the coil, I the current in amperes, A the cross-sectional area of the coil, F the force

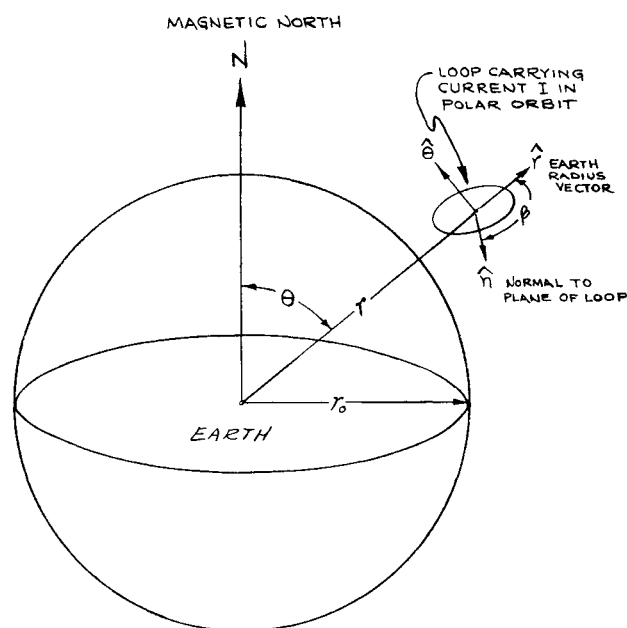


Fig. 1 Acceleration of magnetic dipole in polar orbit.

Received February 5, 1964. The author wishes to acknowledge the valuable consultation of Donald E. Anderson, University of Minnesota, in formalizing the magnetic dipole concept and in evaluating the prospects for the use of superconductor.

* President.